

# Simple fluid models for super-inflation in effective LQC and effects on the CMB B-modes

J. Ribassin,<sup>\*</sup> E. Huguet,<sup>†</sup> and K. Ganga<sup>‡</sup>  
*APC - Astroparticule et Cosmologie (UMR 7164),  
 Université Paris Diderot-Paris 7,  
 10, rue Alice Domon et Léonie Duquet F-75205 Paris Cedex 13, France*

Loop quantum cosmology allows to replace the original singularity by a quantum bounce followed by a phase of fast expansion called super-inflation. In this paper, we use a simple analytic description of super-inflation using the equation of state of a fluid. We then derive the power spectrum of tensor perturbations produced. The effects on the B-mode polarization of the cosmological background radiation are discussed. For a large region of phase space, the spectrum should be distinguishable from the standard inflationary prediction for future observations.

PACS numbers:

## I. INTRODUCTION

The Loop Quantum Cosmology (LQC) [1], [2] (a recent review) is mainly the application to homogeneous spacetimes of the quantization methods of Loop Quantum Gravity (LQG) [3–5], a non-perturbative and background independent canonical quantization of general relativity. A central result of the theory is that the singular evolution encountered in the Wheeler-de Witt theory no longer appears [6, 7]. This is commonly interpreted as the replacement of the big bang singularity by a bounce. That result is a strong motivation to obtain quantitative predictions from LQC as a cosmological scenario. Since a complete quantum solution is not available at present, a constructive means to obtain some insights of the consequences of the phase close to the bounce is that of using effective equations [2, 8]. In such equations, the effects induced by the quantum nature of the geometry are taken into account through corrective terms in classical equations. In isotropic flat models (which are the only models considered here) two main corrections are used : the "inverse volume correction" which comes from the spectra of the quantum operator related to inverse triads, and the "holonomy correction" coming from the quantization scheme in which holonomy of the connection are basic variables. The relative importance of the two type of corrections is still under discussion, it is then usual to consider their effect separately. In the present work we focus on holonomy corrections and more specifically on the possible effects of the super-inflationary phase (in which the Hubble factor is growing) [10, 11] on the tensor modes of the power spectrum of the CMB. A number of study have already been devoted to tensor mode in LQC [12, 23]. Recently, effect of the big bounce on the B-modes of the CMB has been considered [23] (see also [24] for a different approach), where the matter content

of the universe was taken into account through a massive scalar field. In the present work we modelize the content of the universe during the phase of super-inflation using the simple equation of state  $p = \omega\rho$ , for which the modified Friedmann equation admits solutions in closed form for some relevant values of the constant  $\omega$ . We show that during the super-inflation that equation of state for a massless scalar field ( $\omega = 1$ ) is a very good approximation to the massive scalar field in a fast roll regime ( $\dot{\phi}^2 \gg V(\phi)$ ). We compute in both cases (massless scalar and fast rolling massive scalar) the power spectrum after the phase of super-inflation including the holonomy corrections. We then estimate the B-modes and discuss the sensitivity of the spectrum to the model considered.

In Sec. II we describe the dynamics the of a fluid governed by a simple equation of state  $p = \omega\rho$ . We study how this equation compares with that of a massive scalar during the super-inflationary phase. The primordial and B-mode power spectra for the case  $\omega = 1$  are determined and discussed and compared to the standard inflationary prediction in Sec. III. Except otherwise stated, the geometric units  $\hbar = c = G = 1$  are used throughout the paper.

## II. DYNAMICS OF THE SUPER-INFLATION FROM A SIMPLE FLUID MODEL

We assume that the dynamics of the universe is described by the LQC modified Friedmann equation [9]:

$$H^2 = \frac{\kappa}{3}\rho \left(1 - \frac{\rho}{\rho_c}\right), \quad (1)$$

where  $\kappa = 8\pi G$  and  $\rho_c$  is the so-called critical density. The modified Friedmann equation (1) captures the ultraviolet corrections arising from the discrete quantum geometric effects. In particular, we see that when  $\rho = \rho_c$  the theory departs drastically from general relativity: the Hubble parameter vanishes, and the Universe experiences a turnaround in the scale factor. The Big Bang singularity is therefore avoided and replaced by a big bounce.

<sup>\*</sup>Electronic address: ribassin@apc.univ-paris7.fr

<sup>†</sup>Electronic address: huguet@apc.univ-paris7.fr

<sup>‡</sup>Electronic address: ganga@apc.univ-paris7.fr

The critical density can be expressed as a function of the so-called Barbero-Immirzi parameter  $\gamma$  [2]:

$$\rho_c = \frac{\sqrt{3}}{16\pi^2 G^2 \gamma^3 \hbar} \approx 0.82 \rho_{\text{Pl}}. \quad (2)$$

Combining (1) with the derivative of the continuity equation  $\dot{\rho} + H(\rho + p) = 0$  leads to

$$\dot{H} = -\frac{\kappa}{3}(\rho + p) \left(1 - 2\frac{\rho}{\rho_c}\right),$$

which shows that for  $p \geq 0$  the Hubble factor increases between the bounce ( $\rho = \rho_c$ ) and  $\rho = \rho_c/2$ . This is the phase of super-inflation.

As for most non linear equations, it is often impossible to find an exact solution of the modified Friedmann equation. However, with the generic equation of state  $p = \omega\rho$ , which, using the equation for the energy conservation, translates in  $\rho = \xi a^{-X}$ , where  $\xi$  and  $X = 3(1+\omega)$  are constants and  $a$  is the scale factor, the modified Friedmann equation becomes

$$\dot{a}^2 = \frac{\kappa}{3} \xi a^{2-X} \left(1 - \xi \frac{a^{-X}}{\rho_c}\right). \quad (3)$$

This equation can be solved literally for certain values of  $X$ , in particular for  $X = 0$  (inflation or cosmological constant),  $X = 2$  (unknown fluid),  $X = 4$  (ultra-relativistic matter) and also (not so easily) for  $X = 6$  (massless scalar field).

The boundary condition for the modified Friedmann equation is given at the bounce, where the density reaches the critical density. Thus  $\xi = \rho_c a_0^X$ , where  $a_0$  is (chosen to be) the first eigenvalue of the scale factor which, according to [29], is:

$$a_0 = \frac{3\sqrt{\kappa}}{128\sqrt{\pi}(\sqrt{2}-1)}.$$

Note that, we can also determine thanks to (3) the value of the scale factor at the end of super-inflation ( $\rho = \rho_c/2$ ) for  $X > 0$ :

$$a_{\text{end}} = 2^{\frac{1}{X}} a_0,$$

thus, the number of e-folds of super-inflation is simply given by:

$$N = \frac{\ln(2)}{X}.$$

It is then clear that for  $X > 1$  super-inflation alone won't give a decent amount of e-folds.

In order to compare with the case of a single massive scalar field one can rewrite the equation of state for the scalar field under the form  $p = \omega\rho$  with  $\omega$  and thus

$X$  time dependant. Since the evolution of the scalar field is as usual governed by the Klein-Gordon equation

$$\ddot{\phi} + 3H\dot{\phi} + m^2\phi = 0. \quad (4)$$

By restricting the study to the case where the back-reaction is negligible [26], one can solve numerically this equation together with the modified Friedmann eq. (1) to obtain the field  $\phi(t)$ . Then, from the expression of the pressure and the density of a scalar field, namely

$$p = \frac{1}{2}(\dot{\phi}^2 - m^2\phi^2),$$

$$\rho = \frac{1}{2}(\dot{\phi}^2 + m^2\phi^2),$$

one obtains

$$X(t) = \frac{6\dot{\phi}^2}{\dot{\phi}^2 + m^2\phi^2} \quad (5)$$

which is here a function of the time which depends on two physical parameters:  $m$  and  $F_B = m^2\phi(0)^2/2\rho_c$ . It is pictured in Fig. 1.

The evolution of  $X(t)$  shows three main phases: a pre-inflationary phase ( $0 < t < 10^3$ ) during which  $X \approx 6$ , an intermediate phase ( $10^3 < t < 2 \cdot 10^4$ ) during which  $X(t)$  decreases and finally a phase of slow-roll inflation. The length of the pre-inflationary phase is related to the value of  $F_B$ : if the potential energy at the bounce is small, it will take longer to reach a slow rolling regime. During this pre-inflationary phase the dynamic of the massive scalar field can be approximated by the simple fluid  $p = \omega\rho$  with  $\omega = 1$  ( $X = 6$ ). Such an equation of state corresponds to a massless scalar field. A more accurate description of this phase can be obtained with a fast rolling scalar field, i.e. such that  $\dot{\phi}^2 \gg V(\phi)$ , with equation of state  $X(t) \approx 6$ . In what follows we will study these two approximations. Note that the time  $t_{\text{end}}$  at which the super-inflation ends is easily determined from  $\rho(t)$  (Fig. 2) thanks to the relation  $\rho(t_{\text{end}}) = \rho_c/2$ . One observes that the super-inflation represents a very small fraction of the pre-inflationary phase.

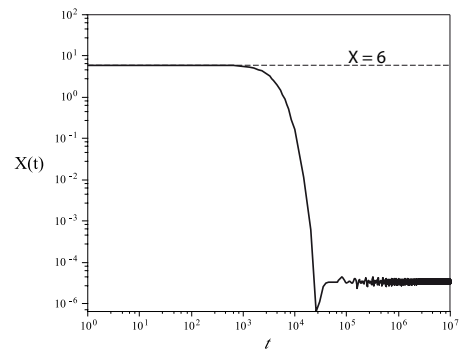


FIG. 1: Evolution of  $X(t)$  for  $m = 6 \cdot 10^{-7}$  and  $F_B = 10^{-9}$ .

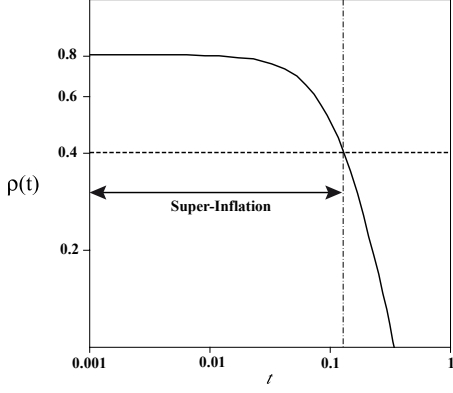


FIG. 2: Evolution of  $\rho(t)$  for  $m = 6.10^{-7}$  and  $F_B = 10^{-9}$ . The horizontal dashed line represents the value at which super-inflation ends. Here super-inflation lasts a bit more than 0.1 and thus  $10^4$  times less than the phase with  $X \approx 6$ .

Let us now turn to the tensor modes. From the considerations of the previous paragraph, one can assume that the matter is described by a scalar and then consider the two approximations (massless and fast roll) for the pre-inflationary phase. In order to obtain the power spectra of the perturbations, we have to solve the equation of propagation of the tensor modes, which can be written as

$$u_k''(\eta) + \left( k^2 + m_{holo}^2(\eta) - \frac{a''(\eta)}{a(\eta)} \right) u_k(\eta) = 0, \quad (6)$$

where  $m_{holo}^2$  is the holonomy correction [25]

$$m_{holo}^2(\eta) = 2\kappa a^2(\eta) \frac{\rho}{\rho_c} \left( \frac{2}{3}\rho - V(\phi) \right). \quad (7)$$

Thanks to (5),  $V(\phi)$  can be written as function of  $X$ :

$$V = \xi a^{-X} \left( 1 - \frac{X}{6} \right), \quad (8)$$

and thus

$$m_{holo}^2 = \frac{2\kappa}{\rho_c} \xi^2 a^{2-2X} \frac{X-2}{6}. \quad (9)$$

We now determine the two quantities  $m_{holo}^2$  and  $a''(\eta)/a(\eta)$  for each approximation: free massless and fast rolling scalar.

#### A. Free Massless scalar field ( $X=6$ )

The modified Friedmann equation can be written as:

$$(\dot{a}^2)^2 = \frac{4\kappa\xi}{3a^2} \left( 1 - \frac{\xi}{a^6\rho_c} \right), \quad (10)$$

its solution is then:

$$a^6(t) = \frac{\xi}{\rho_c} (1 + \kappa\rho_c(t-d)^2), \quad (11)$$

where  $d$  is a constant determined by the initial conditions. At  $t = 0$ , one gets

$$a_0^6 = \frac{\xi}{\rho_c} = \frac{\xi}{\rho_c} (1 + \kappa\rho_c d^2), \quad (12)$$

which implies that  $d = 0$ . The conformal time is then given by

$$\begin{aligned} \eta(t) &\equiv \int \frac{dt}{a(t)} \\ &= \left( \frac{\rho_c}{\xi} \right)^{\frac{1}{6}} t {}_2F_1\left(\frac{1}{6}, \frac{1}{2}; \frac{3}{2}, -\kappa\rho_c t^2\right) \\ &= \frac{1}{a_0} t + o(t^2), \end{aligned} \quad (13)$$

where  ${}_2F_1(n; d; z)$  is a hypergeometric function.

One can compute the terms of the propagation equation:

$$m_{holo}^2 = \frac{4\kappa}{3\rho_c} \xi^2 a^{-10} = \frac{4\kappa}{3} \left( \frac{\rho_c}{\xi} \right)^{\frac{1}{3}} (1 + \kappa\rho_c t^2)^{-\frac{5}{3}} \quad (14)$$

and

$$\frac{a''}{a} = -\frac{\kappa\xi^{1/3}}{27} \rho_c^{2/3} (2\kappa\rho_c t^2 - 3) \frac{3\kappa\rho_c t^2 + \kappa\rho_c t + 3}{(1 + \kappa\rho_c t^2)^{\frac{8}{3}}}. \quad (15)$$

#### B. Fast rolling scalar field ( $X \approx 6$ )

For a fast rolling scalar field ( $\frac{1}{2}\dot{\phi}^2 \gg V(\phi)$ ), the Friedman (1) and Klein Gordon (4) equations reduce to:

$$H^2 = \frac{\kappa}{6} \dot{\phi}^2 \left( 1 - \frac{\dot{\phi}}{2\rho_c} \right), \quad (16)$$

$$\ddot{\phi} + 3H\dot{\phi} = 0. \quad (17)$$

Thus

$$\ddot{\phi}^2 = \frac{\kappa}{6} \dot{\phi}^4 \left( 1 - \frac{\dot{\phi}}{2\rho_c} \right), \quad (18)$$

whose solution is

$$\dot{\phi}(t) = \sqrt{\frac{6\rho_c}{3 + \kappa\rho_c(t-A)^2}} \quad (19)$$

where  $A$  is a constant fixed by the initial conditions. At  $t = 0$ ,  $\rho = \rho_c = \frac{1}{2}\dot{\phi}^2$  and so one gets

$$\dot{\phi}(0) = \sqrt{2\rho_c} = \sqrt{\frac{6\rho_c}{3 + \kappa\rho_c A^2}} \quad (20)$$

which implies that  $A = 0$ . Using the Friedman equation, one can then derive the Hubble parameter:

$$H(t) = -\frac{1}{6} \frac{\kappa\rho_c t}{3 + \kappa\rho_c t^2} \quad (21)$$

and since  $H = \dot{a}/a$ , the scale parameter is:

$$a(t) = a_0 \left( \frac{1}{1 + \frac{\kappa\rho_c}{3} t^2} \right)^{\frac{1}{6}}. \quad (22)$$

As in the previous case, the conformal time takes the form

$$\begin{aligned} \eta(t) &\equiv \int \frac{dt}{a(t)} \\ &= \frac{1}{a_0} t {}_2F_1\left(\frac{1}{6}, \frac{1}{2}; \frac{3}{2}, -\kappa\rho_c t^2\right) \\ &= \frac{1}{a_0} t + o(t^2). \end{aligned} \quad (23)$$

We can compute the terms of the propagation equation:

$$m_{holo}^2 = \frac{\kappa}{3\rho_c} a^2 \dot{\phi}^4 = 3^{\frac{1}{3}} \frac{12 \kappa\rho_c a_0^2}{(3 + \kappa\rho_c t^2)^{\frac{7}{3}}} \quad (24)$$

and

$$\frac{a''}{a} = 3^{\frac{1}{3}} \frac{\kappa\rho_c a_0^2}{9} \frac{5\kappa\rho_c t^2 - 9}{(3 + \kappa\rho_c t^2)^{\frac{7}{3}}}, \quad (25)$$

which are, contrary to the conformal time, slightly different from those obtained for the massless scalar field.

### III. POWER SPECTRA

#### A. super-inflation and beyond

Let us consider the power spectra of the super-inflation alone. For both our modelisations, the equation of propagation of the tensor modes admits no exact solution and was thus solved numerically using a Runge-Kutta method. the power spectra could then be expressed as:

$$P(k) = \frac{k^3}{2\pi^2} \left| \frac{u_k(\eta_{end})}{a(\eta_{end})} \right|^2, \quad (26)$$

where  $\eta_{end}$  corresponds to the end of the pre-inflationary phase ( $t_{end} \approx 10^3$ , see Fig. 1). Thus, we are not only computing the perturbations produced during super-inflation but also those emerging from the intermediate phase that takes place just before the slow-roll regime.

In both cases (Fig. 3 and 4), the slope at large scales grows like  $k^3$  and the spectra begin to oscillate very slightly around  $k = 10^{-2}$ . The minor differences between the two spectra can be ignored (see Fig. 5) as they would be undistinguishable at the scale of the CMB. We therefore conclude that a simple massless scalar field is suitable to describe the perturbations produced by super-inflation.

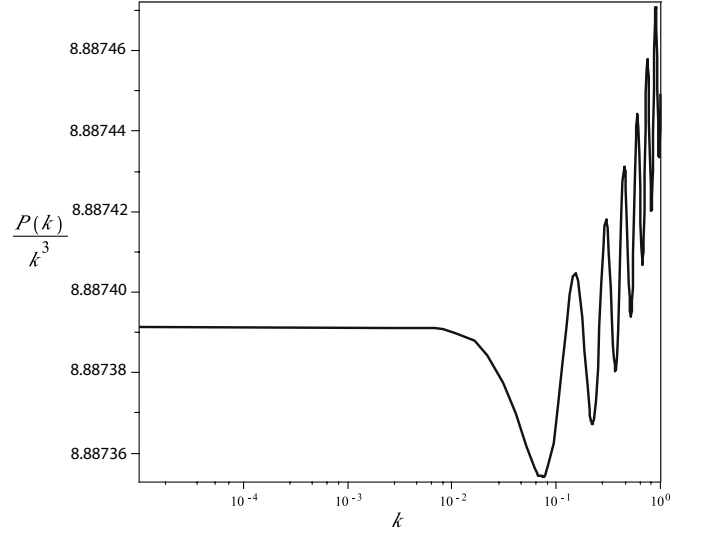


FIG. 3: Power spectrum of the pre-inflationary phase modeled as a massless scalar field ( $X = 6$ ).

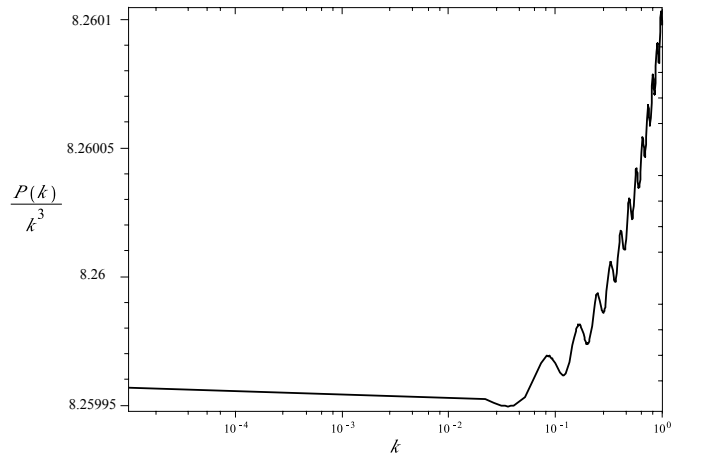


FIG. 4: Power spectrum of the pre-inflationary phase modeled as a fast rolling scalar field ( $X \approx 6$ ).

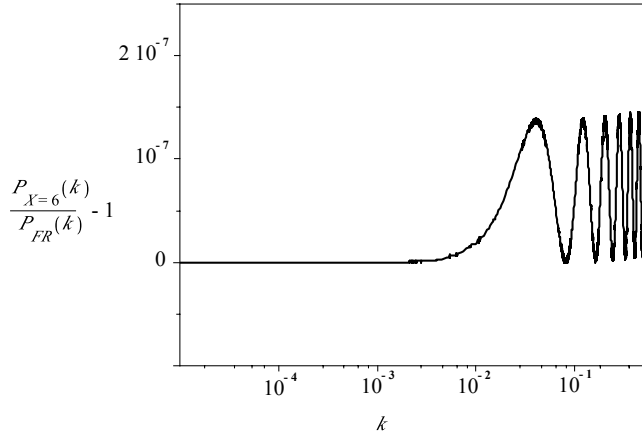


FIG. 5: Comparison between the power spectra in the fast-roll and  $X = 6$  cases.

### B. Complete spectrum of perturbations

To obtain the power spectrum corresponding to the total primordial epoch we have to connect the perturbations that arise from the pre-inflationary phase to a phase of standard slow-roll inflation. To this end we assume that we neglect the perturbations produced during the transition between the two main phases. We also consider that the quantum corrections are negligible during inflation since  $\rho \ll \rho_c$  [26]. The perturbations produced during inflation thus take the usual form

$$v_k(\eta) = -C_1 \sqrt{\frac{\pi\eta}{4}} H_{\frac{3}{2}}^{(1)}(-k\eta) - C_2 \sqrt{\frac{\pi\eta}{4}} H_{\frac{3}{2}}^{(2)}(-k\eta), \quad (27)$$

where  $C_1$  and  $C_2$  are constants and  $H_{\frac{3}{2}}^{(1)}$  and  $H_{\frac{3}{2}}^{(2)}$  Hankel functions of the first and second kind. At the end of the first phase, we impose the continuity of the perturbations and of their first derivative:

$$\begin{aligned} u_k(\eta_{end}) &= v_k(\eta_{end}), \\ u'_k(\eta_{end}) &= v'_k(\eta_{end}). \end{aligned} \quad (28)$$

We can then produce the power spectrum of  $v_k$  at the "end" of inflation (so that the whole phase would yield 70 e-foldings). As in the case of pre-inflationary phase alone, the power spectra (Fig. 6 and 7) still behave like  $k^3$  at large scales. For large  $k$  the spectra are nearly scale invariant as one would expect with inflation. Some oscillations appear between those two regimes. Lowering the value of the parameter  $F_B$  increases the amplitude of these oscillations which thus appear as the consequence of the bounce. As seen in Sec. II, decreasing  $F_B$  increases the length of the pre-inflationary phase, thus giving more time to the holonomy correction to modify the spectrum of perturbations.

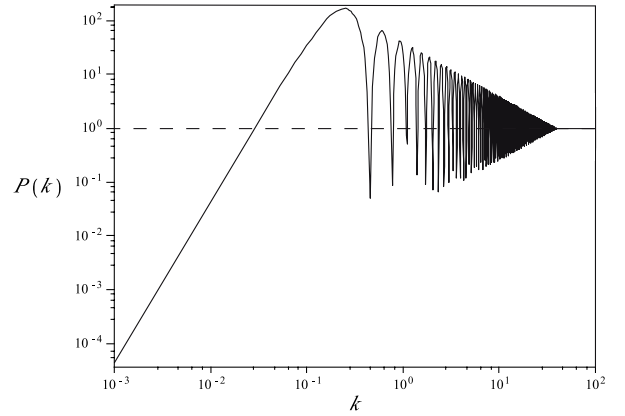


FIG. 6: Power spectrum of the pre-inflationary phase followed by inflation for  $m = 6.10^{-7}$  and  $F_B = 10^{-9}$ . As usual only the super-Hubble modes are considered.

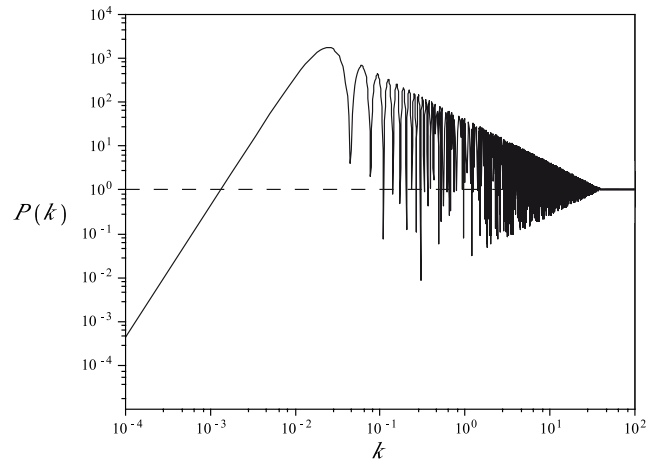


FIG. 7: Power spectrum of the pre-inflationary phase followed by inflation for  $m = 6.10^{-7}$  and  $F_B = 10^{-11}$ . As usual only the super-Hubble modes are considered.

### C. B-mode angular power spectrum

Since we have computed the power spectrum of the tensor perturbations, we are now able to produce the primordial part of the B-mode angular power spectrum of polarization of the CMB. We do not know the modification of the spectrum of scalar perturbations produced by the holonomy correction, we will thus assume that scalar perturbations are given by the usual nearly scale invariant spectrum. This will allow us to produce the part of the spectrum that emerges from the conversion from E-modes to B-modes through lensing. Moreover, the holonomy correction is an ultraviolet correction while the lensed part of the BB angular spectrum is supposed to dominate mostly at small angular scales.

The B-mode power spectra are obtained using CAMB [27]. For the cosmological parameters, we took those

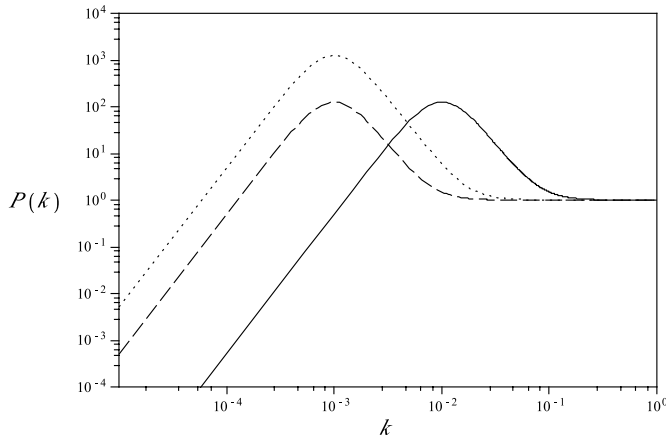


FIG. 8: Parametrization of the primordial power spectrum given by equation (29) with  $(k_0, R) = (10^{-2}, 500)$  (solid),  $(k_0, R) = (10^{-3}, 500)$  (dashed) and  $(k_0, R) = (10^{-3}, 5000)$  (dotted).

given for  $\Lambda$ CDM by WMAP+BAO+H0 [28]. As input for the primordial power spectrum we used a simple parametrization of the previous spectrum inspired by [23]

$$P(k) = \left(\frac{H}{2\pi}\right)^2 \frac{1}{1 + \left(\frac{k_0}{k}\right)^3} \left(1 + \frac{R}{1 + \left(\frac{k}{k_0}\right)^3}\right). \quad (29)$$

The parameters  $k_0$  and  $R$  respectively determine the position and amplitude of the transition between two regimes (Fig. 8):  $P(k) \propto k^3$  at large scale and the spectrum is scale invariant at lower scales. The transition between those two regimes presents a bump. We will not take into account the oscillations of the primordial spectrum in the rest of the computation and only focus on the envelope. The parameter  $R$  is closely related to the parameter  $F_B$ : high values of  $R$  correspond to small values of the potential energy of the scalar field at the bounce. The link between the phenomenological parameter  $k_0$  and the physical parameters is less simple since the position of the bump depends on both  $F_B$  and the length of the slow-roll phase.

The resulting B-mode power spectra are presented as a function of the parameter  $k_0$  in Fig. 9 and 10 with tensor-scalar ratios of  $10^{-1}$  and  $10^{-2}$  respectively. At large multipole, the spectra are dominated by the contribution of the lensing as in the usual scenario and are thus independent of  $k_0$ . However, the spectra also reach a maximum in two regions: at large angular scales ( $\ell < 10$ ) for  $k_0 < 10^{-3}$  and at intermediate scales ( $20 < \ell < 200$ ) for values of  $k_0$  around  $10^{-2}$ . The latter case is the most interesting from an observational point of view since it coincides with the beginning of the observational window of ground based experiments like BICEP [30].

An important question is whether future experiments would be able to discriminate between B-modes produced by inflation and B-modes arising from a bouncing cosmology.

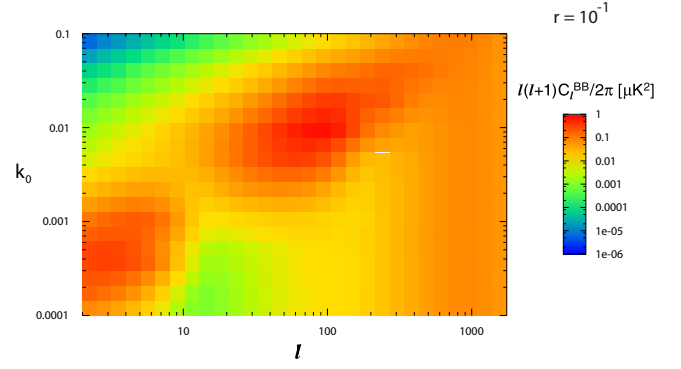


FIG. 9: Angular power spectrum of the B modes as a function of  $k_0$  with a tensor-scalar ratio of  $10^{-1}$  and  $R = 500$ .

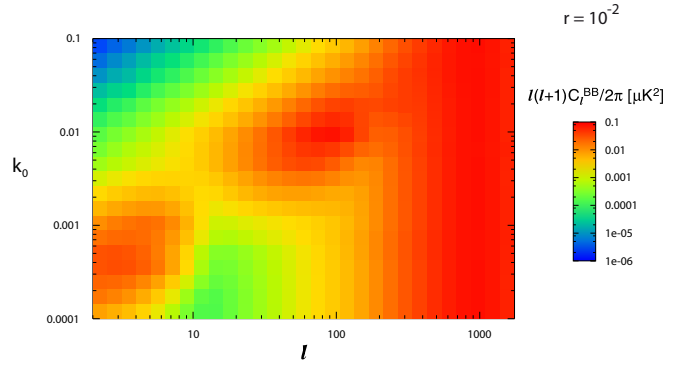


FIG. 10: Angular power spectrum of the B modes as a function of  $k_0$  with a tensor-scalar ratio of  $10^{-2}$  and  $R = 500$ .

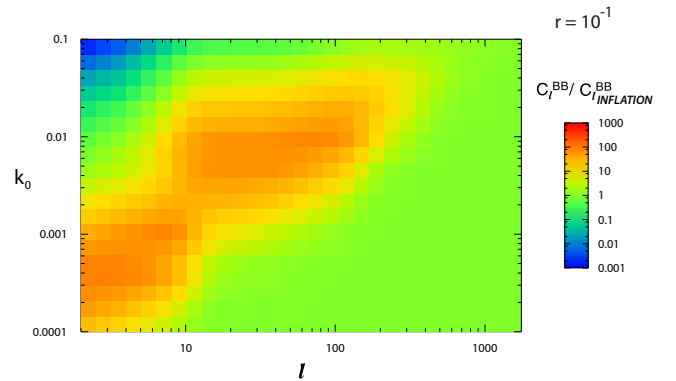


FIG. 11: Angular power spectrum of the B modes divided by the standard inflationary prediction as a function of  $k_0$  with a tensor-scalar ratio of  $10^{-1}$  and  $R = 500$ .

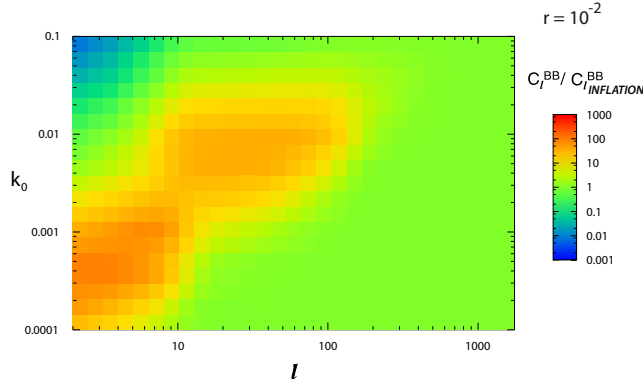


FIG. 12: Angular power spectrum of the B modes divided by the standard inflationary prediction as a function of  $k_0$  with a tensor-scalar ratio of  $10^{-2}$  and  $R = 500$ .

ogy in the framework of LQC. A global analysis on all multipoles of a similar model was performed in [23] using a Fisher analysis method to determine the detectability of the bump of the primordial spectrum of gravitational waves. Here we will take a complementary point of view, we will determine the multipoles where the B-modes arising from LQC can be distinguished from those produced by a standard inflationary scenario. In Fig. 11 and 12 are presented the B-mode power spectra divided by the standard inflationary prediction as a function of the parameter  $k_0$  with tensor-scalar ratios of  $10^{-1}$  and  $10^{-2}$  respectively. Due to the contribution of the lensing, the LQC and inflationary spectra are identical at small angular scales. However, for multipoles smaller than 200 the LQC spectra show significant departures from the standard inflationary prediction for identical tensor-scalar ratios in the two regions described previously. For  $R = 500$ , which corresponds to the primordial spectrum of Fig. 6 with  $F_B = 10^{-9}$ , those departures can reach two orders of magnitude for  $k_0 \approx 10^{-2}$ . The corresponding angular power spectra are presented in Fig. 13 and 14. In the following we will only focus on spectra obtained for  $k_0 = 10^{-2}$  since it corresponds to the region of the parameter space where the models can be most easily distinguished.

For high values of  $R$  the spectra are very different from the inflationary spectra as they possess a peak around  $\ell = 100$  which should allow to discriminate between the models. In fact in the case of a tensor-scalar ratio  $r$  of  $10^{-1}$ , a large region of phase space is even already excluded by the BICEP data [30] (see Fig. 13). For smaller tensor-scalar ratios like  $r = 10^{-2}$  only high values of  $R$  are excluded by the data. For smaller values of  $R$  and thus for higher values of  $F_B$  the spectra come closer to the inflationary prediction in the observable range ( $\ell > 20$ ), especially for low values of the tensor-scalar ratio. Nevertheless, the importance of the backreaction [31] grows as  $F_B$  gets bigger and the effective model of LQC that we

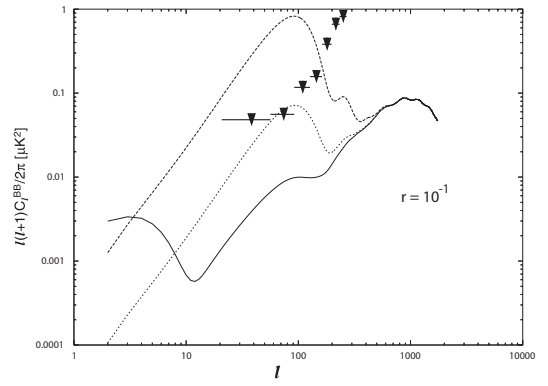


FIG. 13: B modes for  $R = 50$  (dashed),  $R = 500$  (long dashed) and  $k_0 = 10^{-2}$  for a tensor-scalar ratio of  $10^{-1}$ . The solid line corresponds to the prediction of inflation with a tensor-scalar ratio of  $10^{-1}$ . The 95% confidence upper limits on the detection of B-modes of polarization given by BICEP [30] are also pictured.

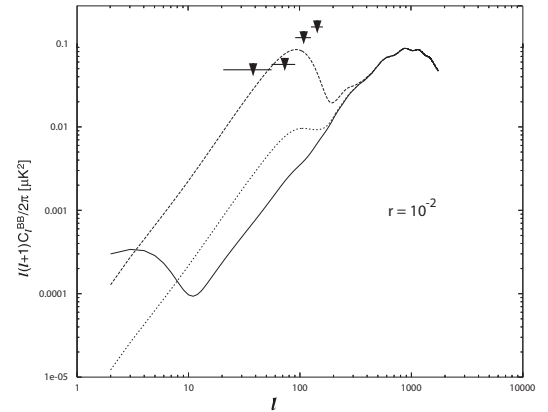


FIG. 14: B modes for  $R = 50$  (dashed),  $R = 500$  (long dashed) and  $k_0 = 10^{-2}$  for a tensor-scalar ratio of  $10^{-2}$ . The solid line corresponds to the prediction of inflation with a tensor-scalar ratio of  $10^{-2}$ . The 95% confidence upper limits on the detection of B-modes of polarization given by BICEP [30] are also pictured.

are using here is no more valid. Therefore our conclusions only concern relatively large values of  $R$ .

The situation changes as the tensor-scalar ratio decreases and the inflationary and LQC spectra might be indistinguishable. In Fig. 15 not only is the gap between the inflationary and LQC spectra for  $r = 10^{-3}$  much smaller than in the  $r = 10^{-1}$  or  $r = 10^{-2}$  cases but the LQC spectrum for  $r = 10^{-3}$  also yields the same B-modes as inflation with  $r = 10^{-1}$  in the observable range ( $\ell > 20$ ). This arises from the fact that the LQC spectra no longer possess a peak at low tensor-scalar ratios but a plateau around  $\ell = 100$  which is similar to the one present in the inflationary spectrum. The B-modes of polarization produced in the frame work of LQC should thus be distinguishable in the observable



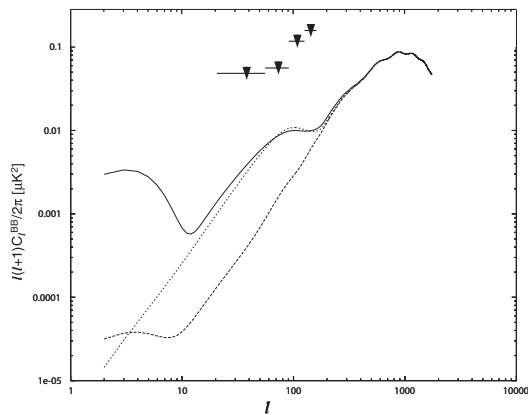


FIG. 15: B modes for  $R = 500$  (long dashed) and  $k_0 = 10^{-2}$  for a tensor-scalar ratio of  $10^{-3}$ . The solid and dashed lines correspond respectively to the predictions of inflation with tensor-scalar ratios of  $10^{-1}$  and  $10^{-3}$ . The 95% confidence upper limits on the detection of B-modes of polarization given by BICEP [30] are also pictured.

range of multipoles from the inflationary prediction for low values of the potential energy at the bounce and for moderate tensor-scalar ratios. Therefore, future satellite and ground-based experiments should either be able to discriminate between LQC and inflation or to strongly constrain the effective model of LQC used in this study.

- 
- [1] M. Bojowald, *Living Rev. Relativity* **11**, 04 (2008).
  - [2] A. Ashtekar and P. Singh, *Class. Quant. Grav.* **28**, 213001 (2011).
  - [3] T. Thiemann, *Introduction to Modern Canonical Quantum General Relativity*, Cambridge University Press (2007).
  - [4] C. Rovelli, *Quantum Gravity*, Cambridge University Press (2004).
  - [5] A. Ashtekar and J. Lewandowski, *Class. Quant. Grav.* **21**, R53 (2004).
  - [6] M. Bojowald, *Phys. Rev. Lett.* **86**, 5227, (2001).
  - [7] M. Bojowald, *Phys. Rev. Lett.* **100**, 221301, (2008).
  - [8] A. Ashtekar, T. Pawłowski and P. Singh, *Phys. Rev. D* **73**, 124038 (2006).
  - [9] A. Ashtekar, T. Pawłowski and P. Singh, *Phys. Rev. D* **74**, 084003 (2006).
  - [10] M. Bojowald, *Phys. Rev. Lett.* **89**, 261301, (2002).
  - [11] P. Singh, *Phys. Rev. D* **73**, 063508 (2006).
  - [12] D. Mulryne and N. Nunes, *Phys. Rev. D* **74**, 083507 (2006).
  - [13] J. Mielczarek and M. Szydlowski, *Phys. Lett. B* **657**, 20 (2007).
  - [14] E. J. Copeland, D. J. Mulryne, N. J. Nunes and M. Shaeri, *Phys. Rev. D* **77**, 023510 (2008).
  - [15] J. Mielczarek, *J. Cosmol. Astropart. Phys.* **11**, 011 (2008).
  - [16] E. J. Copeland, D. J. Mulryne, N. J. Nunes and M. Shaeri, *D* **79**, 023508 (2009).
  - [17] J. Mielczarek, *Phys. Lett. B* **675**, 273 (2009).
  - [18] J. Mielczarek, *Phys. Rev. D* **79**, 123520 (2009).
  - [19] J. Grain and A. Barrau, *Phys. Rev. Lett.* **102**, 081301 (2009).
  - [20] M. Shimano and T. Harada, *Phys. Rev. D* **80**, 063538 (2009).
  - [21] J. Grain, A. Barrau, and A. Gorecki, *Phys. Rev. D* **79**, 084015 (2009).
  - [22] J. Grain, T. Cailleteau, A. Barrau and A. Gorecki, *Phys. Rev. D* **81**, 024040 (2010).
  - [23] J. Grain, A. Barrau, T. Cailleteau and J. Mielczarek, *Phys. Rev. D* **82**, 123520 (2010).
  - [24] Y.-Z. Ma, W. Zhao, and M. L. Brown, *J. Cosmol. Astropart. Phys.* **10**, 007 (2010).
  - [25] M. Bojowald and G. M. Hossain, *Phys. Rev. D* **77**, 023508 (2008).
  - [26] A. Ashtekar and D. Sloan, *Phys. Lett. B.* **694**, 108 (2010).
  - [27] A. Lewis, A. Challinor and A. Lasenby, *Ap. J.* **538**, 473 (2000).
  - [28] E. Komatsu et al., *Astrophys. J. Suppl.* **192**, 18 (2011).
  - [29] M. Bojowald, [arXiv:gr-qc/0305069v1].
  - [30] H. C. Chiang, *Astrophys. J.* **711**, 1123 (2010).
  - [31] M. Bojowald, A. Skirzewski, *Int. J. Geom. Meth. Mod. Phys.* **4**, 25 (2007).